Future Prospects for Defect and Strain Analysis in the SEM via Electron Channeling

Yoosuf N. Picard,[1] * Ranga Kamaladasa,[1] Marc De Graef,[1] Noel T. Nuhfer,[1] William J. Mershon,[2] Tony Owens,[2] Libor Sedlacek,[3] and Filip Lopour[3]

[1]Department of Materials Science and Engineering, Carnegie Mellon University, Pittsburgh, PA 15213
[2]TESCAN USA Inc., 508 Thomson Park Drive, Cranberry Township, PA 16066
[3]TESCAN, a.s., Libusina tr. 21, 623 00, Brno, Czech Republic

* ypicard@cmu.edu

Editor's Note: This article relates to the MAS Topical Conference, Electron Backscatter Diffraction (EBSD), to be held June 19–21, 2012, at Carnegie Mellon University, Pittsburgh, PA. For a description go to: www.microbeamanalysis.org.

Introduction

Electron diffraction in both SEM and TEM provides a contrast mechanism for imaging defects as well as a means for quantifying elastic strain. Electron backscatter diffraction (EBSD) is the commercially established method for SEM-based diffraction analysis. In EBSD, Kikuchi patterns are acquired by a charge-coupled device (CCD) camera and indexed using commercial software. Phase and crystallographic orientation information can be extracted from these Kikuchi patterns, and researchers have developed cross-correlation methods to measure strain as well [1].

SEM-based electron channeling is an alternative diffraction method to EBSD. Electron channeling refers to the variation in backscattered electron (BSE) yield as a function of the relationship between the incident electron beam and the target crystal's orientation. For a crystal imaged at low magnification, the large angular changes in the electron beam's incoming trajectory cause BSE intensity variations and produce a Kikuchi-like pattern, or electron channeling pattern (ECP), superimposed on the crystal [2]. At high magnification, the electron beam incoming trajectory is near-constant during scanning, and any BSE intensity variations will be due to local changes in the crystal's orientation, such as the strain surrounding extended defects. These cases assume a chemically homogeneous crystal, free of topographic features, where the only BSE imaging contrast mechanism is channeling.

Because detection of electron channeling effects simply involves BSE imaging, any commercial SEM equipped with a BSE detector can be used for channeling-based analysis. Defect detection by electron channeling contrast imaging (ECCI) is well established with recent examples in metals [3–6] and semiconductors [7–9]. However, defect identification by ECCI is not well established. Defect identification by TEM employs diffraction contrast and can be accomplished either by using the $g \bullet b = 0$ invisibility criterion or by comparing experimentally acquired images to dynamical diffraction simulations. ECCI-based defect identification should be accessible by the same approaches. This article illustrates various examples where defect identification might be realized. Additionally, this article presents preliminary experimental/simulation comparisons that highlight opportunities for future development and prospects for realizing strain analysis via SEM-based channeling.

Methods and Materials

Four semiconducting materials were analyzed in this study: an epitaxial GaN (0001) film on a sapphire substrate, a commercial $SrTiO_3$ (001) substrate, an epitaxial GaSb (001) film on a GaAs substrate, and Si (001) and (111) substrates. ECCI and ECP acquisition in this study was performed on two SEMs, one with and one without beam rocking capabilities. GaN and $SrTiO_3$ were analyzed in an FEI Quanta 600 FEG SEM at 20 kV accelerating voltage and 3–6 nA beam current. Samples were imaged using a pole-piece-mounted annular solid state BSE detector with an 8.4 mm working distance to optimize BSE collection. GaSb and Si were analyzed in a TESCAN Mira 3 FEG SEM at 20–30 kV accelerating voltage and ~2 nA beam current. A retractable annular YAG scintillator detector was used for BSE imaging at a working distance of 6–8 mm. The Mira 3 includes a channeling mode that can rock the beam about a 10–25 µm region of the specimen surface, providing selected-area ECP (SACP) acquisition.

Results

Dislocation imaging in GaN. GaN is one of many tunable bandgap semiconductors important for solid-state lighting, light-emitting diodes, RF devices, and third generation solar cells. Threading dislocations are defects that extend through the GaN and are associated with diminished electrical and optical performance. ECCI presents a potentially viable means for mapping and quantifying threading dislocations in GaN. Because these defects penetrate the GaN (0001) surface, they can be readily imaged in the SEM by ECCI as shown in Figure 1. A side-by-side comparison of standard secondary electron (SE) imaging and BSE imaging shows the emergence of dark/light spots only in the BSE image. These dark/light spots denote individual threading dislocations. Particles on the surface appear as solid white artifact features in both the SE and BSE images.

Electron channeling contrast imaging requires the specimen to be oriented so that the incoming electron beam trajectory satisfies the Bragg condition for a specific set of planes. Accomplishing this maximizes the channeling contrast so that extended defects, like the dislocations in Figure 1b, appear in the BSE image. The precise incident beam orientation can be selected by tilting/rotating the sample while observing the ECP. In the absence of a beam rocking system, ECPs can be acquired by low-magnification BSE imaging of a single crystal, as shown in Figure 2a. The six-fold symmetry of the GaN (0001) surface is readily apparent in the ECP. As the sample is tilted and/or rotated in the SEM, the ECP translates relative to the crystal surface. Once a channeling line at the edge of

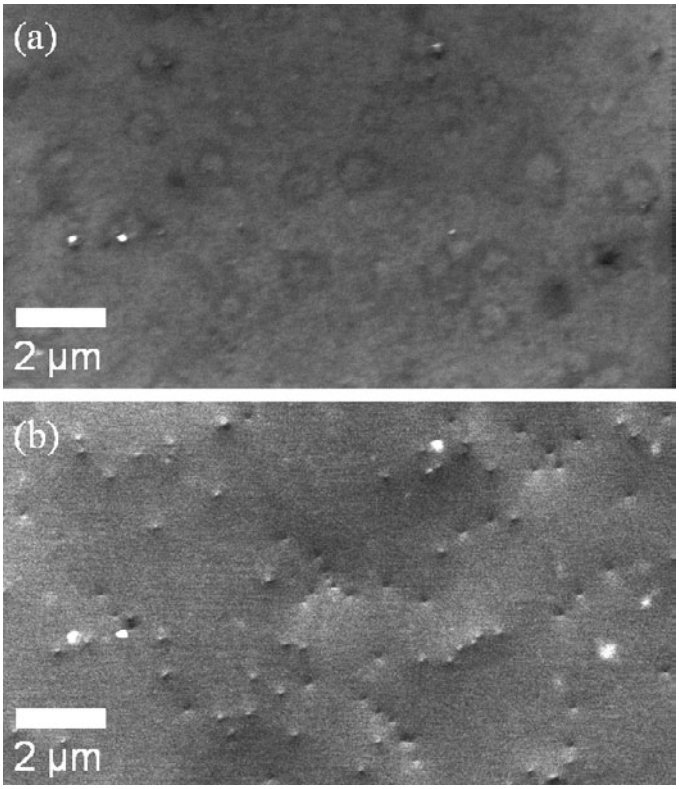

Figure 1: SEM micrographs of a GaN (0001) surface recorded by (a) SE and (b) BSE detection. The BSE image is obtained at a channeling condition; individual extended defects appear as dark/light spots by ECCI.

the band is centered on the optic axis, a diffraction condition or diffraction vector (g) has been selected. This vector lies perpendicular to the channeling line and is normal to the crystallographic planes the channeling line represents. Two diffraction conditions are presented in Figure 2b and 2c, with corresponding ECCI micrographs of the same dislocations for both conditions. The dark/light spots in these micrographs denote screw dislocations penetrating the GaN (0001) surface. The directionality of the dark/light spots appears to rotate 90° as a direct consequence of changing the diffraction condition (or rotating the diffraction vector 90°). This contrast behavior is identical to end-on TEM imaging of screw dislocations and illustrates the similarities between SEM-based ECCI and TEM-based diffraction contrast imaging.

It is important to note that the Burgers vector b, for threading screw dislocations in GaN, is $b = c[0001]$. Assuming the $g \bullet b = 0$ invisibility criterion applies for ECCI as it does for TEM, the dot product of the diffraction vector and the Burgers vector is zero for both imaging conditions in Figure 2b and 2c. Hence, the dislocations should be invisible. However, because the dislocations penetrate a free surface, surface relaxation effects modify the nature of the lattice distortion to create visible contrast for a diffraction condition where contrast is not expected.

Dislocation image invisibility in $SrTiO_3$. $SrTiO_3$ is a useful electrical material and common substrate for other perovskite-structured metal-oxides, materials that exhibit a broad array of multifunctional properties, including ferroelectricity, superconductivity, colossal magnetoresistance, and piezoelectricity. Unwanted intrinsic defects, such as

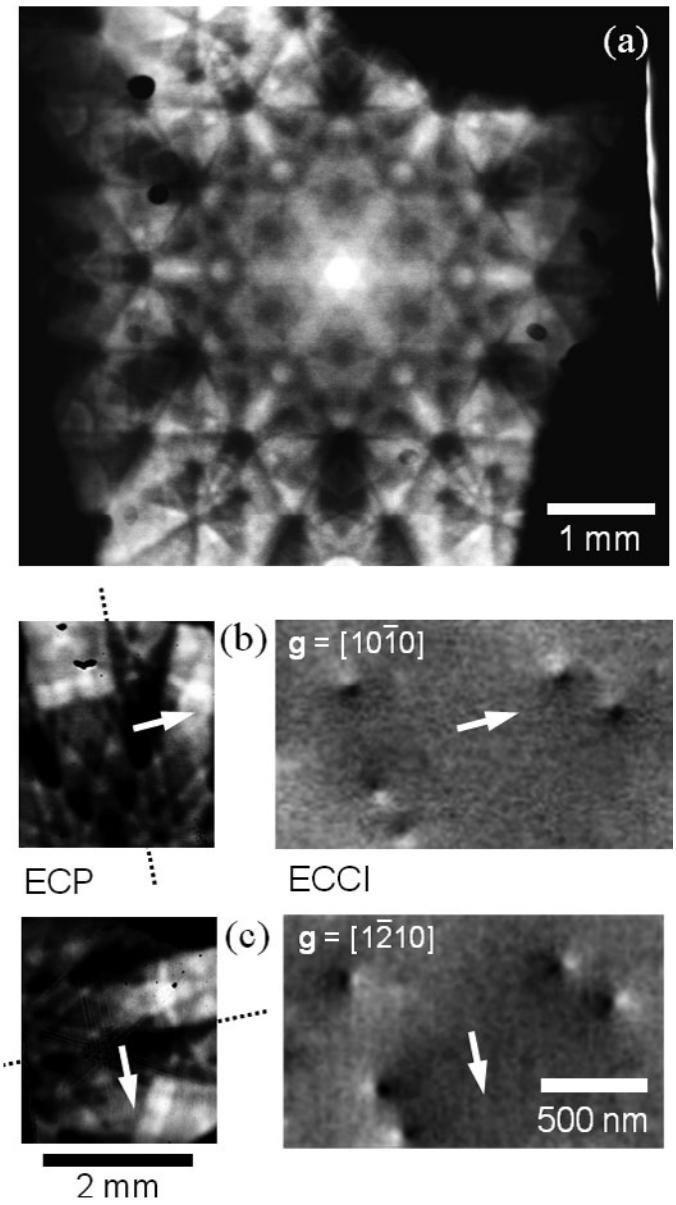

Figure 2: (a) Electron channeling pattern recorded by low-magnification BSE imaging of GaN (0001) surface. The specimen is tilted/rotated so that the electro-optic axis originally centered on the [0001] zone axis (a) is instead centered on the (b) (10–10) or (c) (1–210) channeling line. The corresponding ECCI micrographs for these two channeling conditions show that the screw dislocation contrast directionality depends on the diffraction vector.

dislocation loops, are common in $SrTiO_3$ substrates grown by the Verneuil method [10]. An ECCI micrograph of such defects in $SrTiO_3$ (001) is presented in Figure 3. These defects are {100} half-loops composed of two segments roughly perpendicular to the surface that are connected by a submerged segment roughly parallel to the surface. Pairs of spot features are visible in Figure 3a, denoting dislocation segments perpendicular to and penetrating the surface. A diffuse bright line between each spot pair denotes the submerged, linking dislocation segment. It is interesting that larger spacing between a spot pair corresponds to a more diffuse line feature between the pair, indicative of greater BSE scattering for more deeply submerged dislocations.

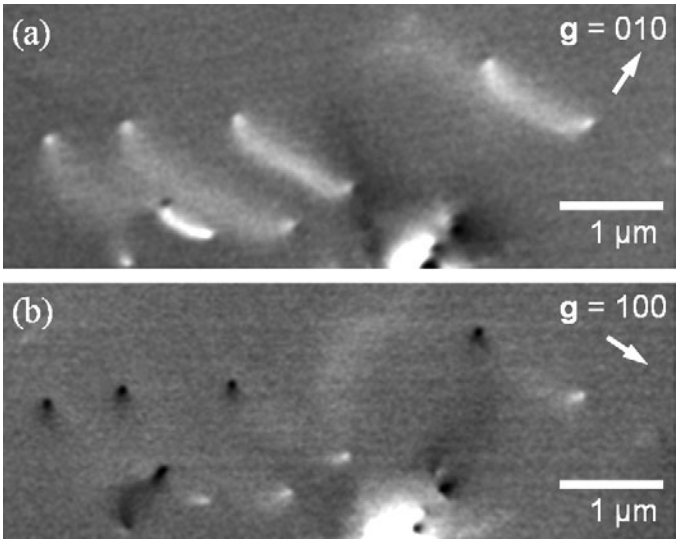

Figure 3: Electron channeling contrast images of a $SrTiO_3$ (001) surface at (a) g = 010 and (b) g = 100 channeling conditions. Subsurface dislocation line segments in (a) become invisible when the diffraction vector is rotated 90° in (b).

When the diffraction vector is rotated 90° (Figure 3b), the submerged dislocation segment is rendered invisible. This observation is consistent with the invisibility criterion because the Burgers vector (b) is now perpendicular to the diffraction vector (g), and thus the dot product of these two vectors is zero. Also, rotation of g has modified the spot features (one spot becoming brighter, the other becoming darker). The opposite nature of the contrast for these two spot features implies opposite line directions, consistent with the expected dislocation loop configuration. In the case of $SrTiO_3$ and GaN, prior knowledge of possible dislocation types and expected dislocation configurations help to guide ECCI interpretation. Image simulations can assist interpretation for those cases where the imaged extended defects are unknown.

Dislocation image simulation for GaSb. GaSb is a narrow bandgap semiconductor important for infrared applications. GaSb-based devices are multilayer structures that can contain various dislocation types that will degrade optoelectronic performance. Figure 4 presents experimental and simulated ECPs and ECCI micrographs for a GaSb (001) film surface. The simulated ECP is generated using a Bloch wave formalism detailed elsewhere [11]. The simulated ECCI micrograph is a calculated solution to the Darwin-Howie-Whelan dynamical scattering equations [12] employing a scattering matrix approach [13]. The simulated micrograph includes ~30 randomly placed dislocations consisting of screw and edge types with line directions ⟨101⟩, ⟨–101⟩ , ⟨011⟩ and ⟨0–11⟩ and Burgers vectors (1/2⟨101⟩ and 1/2⟨011⟩). Comparisons between experimental and simulated patterns/images show good qualitative agreement. The range of dislocation types is broad for GaSb, but many experimental features do match simulated features. Additionally, individual dislocation identification should be possible by matching the exact simulated contrast profile to the dislocation of interest in the experimental ECCI micrograph.

HOLZ lines in Si ECPs. Monocrystalline, polycrystalline, and multicrystalline (large grain) Si are widely used for solar

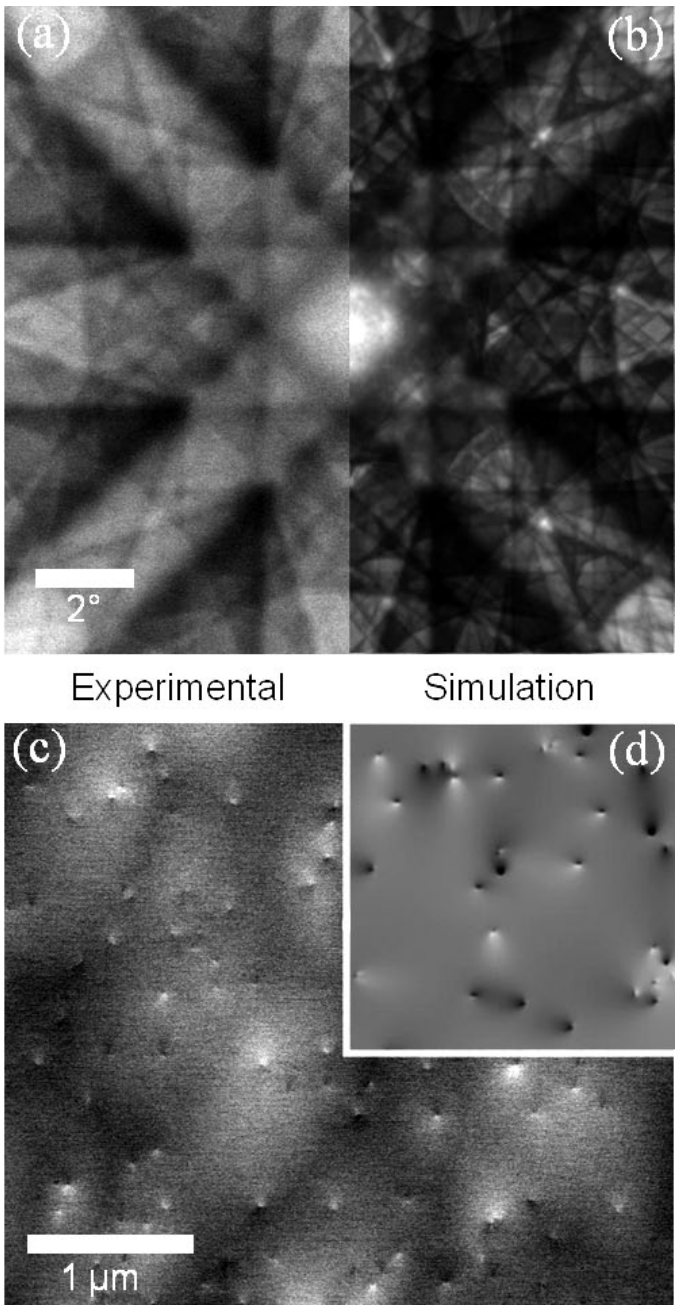

Figure 4: (a) Experimental and (b) simulated ECP of GaSb (001) and (c) experimental and (d) simulated ECCI micrograph of surface penetrating dislocations in GaSb (001).

cells but can be susceptible to processing-induced stresses and impurities. Thus, large area defect and strain mapping techniques are highly desirable. Simulated and experimental ECPs acquired from a Si surface are presented in Figure 5. SEMs equipped with a beam rocking capacity can sample over a large angular range, as demonstrated for Figure 5a. However, the angular range can also be decreased, effectively "magnifying" the ECP about a zone-axis as shown in Figure 5c. This can be done either by decreasing the maximum rocking angle or by increasing the magnification of BSE imaging. Higher-order Laue zone (HOLZ) lines become apparent in the center of the on-zone axis ECP. Because precise lattice

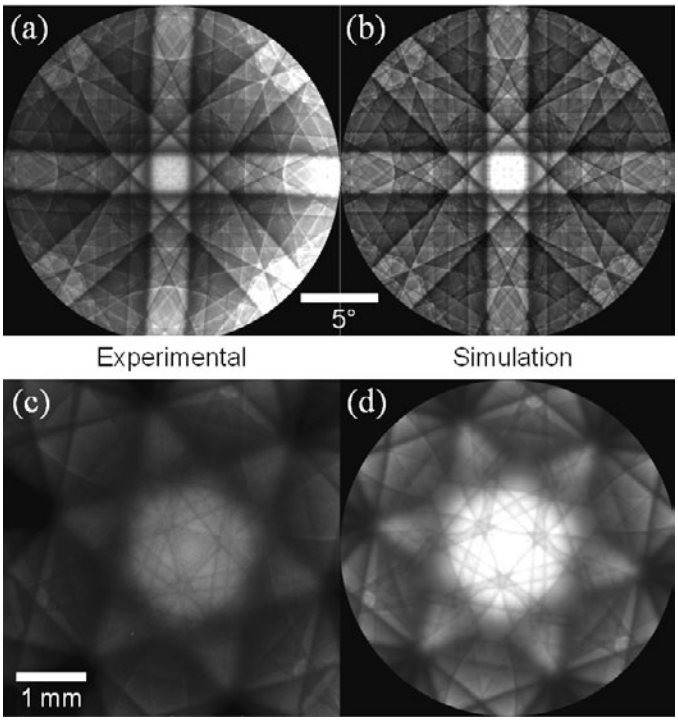

Figure 5: (a) Experimental and (b) simulated electron channeling patterns of Si (001). (c) Experimental and (d) simulated ECPs of Si (111) showing HOLZ lines.

parameter information can be extracted from these HOLZ lines, any resolved angular or translational shift in the HOLZ line positions from one selected area to another is a direct measure of lattice strain. Previous researchers reported 10^{-3} strain sensitivity by this approach [14]. This premise is the basis for strain analysis by TEM-based convergent beam electron diffraction (CBED). Simulations show excellent agreement with the experimental ECPs, including the HOLZ lines.

Future Prospects

Advances in SEM-based channeling applications have relied, and will continue to rely, on instrumentation improvements. Low (<15%) BSE contrast levels require large beam currents (>1 nA) to obtain suitably high signal-to-noise ratios, thus SEM FEG sources are a necessity. Compounded by the beam broadening and diffusion within the material, ECCI/BSE imaging resolution is far worse than conventional SE imaging. These problems can be reduced with more sensitive BSE detectors that lower the beam current requirements, thereby allowing smaller electron probe sizes to be used. Additionally, using lower accelerating voltages should reduce beam broadening and could improve imaging resolution. However, lower accelerating voltages will reduce beam penetration that could sacrifice sensitivity to submerged defects.

Beam rocking, or pivoting about a stationary point on the sample surface, is a useful but rare feature for modern commercial SEMs. The size of the pivot point for commercially available beam rocking systems is on the order of tens of microns. Dynamically corrected rocking can mitigate the spherical aberration of the objective lens and thus achieve a 1 µm selected-area size for SACP [15]. SACP analysis with this spatial resolution is a prerequisite for micron-scale channeling-based strain analysis. Averaged lattice parameter information can be extracted from HOLZ line analysis in a manner similar to TEM-based convergent beam electron diffraction (CBED). Cross-correlation methods [16] could help to resolve HOLZ shifts when comparing neighboring SACPs or comparing individual SACPs to an experimental or simulated "strain-free" reference SACP.

A number of factors will influence the fidelity of HOLZ lines for experimental SACPs. These factors include chromatic aberration, beam divergence, working distance, and angular beam trajectory precision during beam rocking. Depending on the degree of signal loss, energy filtering schemes may serve to enhance HOLZ line quality [17] while also improving ECCI (BSE imaging) resolution [18]. An alternative to SEM beam rocking for SACP acquisition is high precision (<0.1°) tilt rotation, or preferably double-tilt, SEM stages. Because ECCI and ECP involve BSE imaging/acquisition, these methods are susceptible to the same sample surface requirements as EBSD. Surfaces must be topographically smooth (nm to sub-nm root-mean-square roughness) and free of near-surface damage or amorphization. Polished substrates and as-deposited single-crystalline thin films generally have suitable surface quality. Analysis of bulk specimens will require careful mechanical and/or chemical preparation methods to achieve similar surface quality. Finally, electron channeling provides opportunities to exploit the many advantages afforded by the SEM over the TEM. Large area (millimeter-scale) defect/strain mapping is plausible through automated imaging and stage translation. *In-situ* electrical and mechanical studies can take advantage of the large–volume SEM chamber to directly analyze bulk specimens under applied loading.

Conclusion

Technologically relevant materials were analyzed by electron channeling to demonstrate the prospects for reliable defect identification and CBED-like ECP acquisition suitable for strain analysis. Electron channeling contrast images of crystalline defects show contrast behavior similar to that observed in TEM. Simulations based on the Bloch wave formalism and scattering matrix solutions to dynamical electron diffraction equations show good agreement for both ECPs and ECCI micrographs. With continued SEM instrumentation advances and continued research that coordinates experiment with theory, TEM-like analysis methods could become readily available in the SEM for defect and strain analysis.

Acknowledgments

We would like to acknowledge K. Jones (Army Research Laboratory) and G. Balakrishnan (University of New Mexico) for providing specimens. Y. Picard recognizes funding support from the Army Research Office.

References

[1] AJ Wilkinson and D Randman, *Phil Mag* 90 (2010) 1159–77.
[2] DG Coates, *Phil Mag* 16 (1967) 1179–84.
[3] MA Crimp, BA Simkin, and BC Ng, *Phil Mag Lett* 81 (2001) 833–37.
[4] I Gutierrez-Urrutia, S Zaefferer, and D Raabe, *Scripta Mater* 61 (2009) 737–40.
[5] N Kuwano, M Itakura, Y Nagatomo, and S Tachibana, *J Electron Microsc* 59 (2010) S175–81.

[6] A Weidner, S Martin, V Klemm, U Martin, and H Biermann, *Scripta Mater* 64 (2011) 513–16.
[7] C Trager-Cowan, F Sweeney, PW Trimby, AP Day, A Gholinia, NH Schmidt, PJ Parbrook, AJ Wilkinson, and IM Watson, *Phys Rev B* 75 (2007) 085301.
[8] RJ Kamaladasa, F Liu, LM Porter, RF Davis, DD Koleske, G Mulholland, KA Jones, and YN Picard, *J Microsc* 244 (2011) 311–19.
[9] RJ Kamaladasa, WK Jiang, and YN Picard, *J Electron Mater* 40 (2011) 2222–27.
[10] J Nishigaki, K Kuroda, and H Saka, *Phys Status Solidi A* 128 (1991) 319–36.
[11] YN Picard, R Kamaladasa, and M De Graef, in press.
[12] MD Graef, *Introduction to Conventional Transmission Electron Microscopy*, Cambridge University Press, New York, 2003.
[13] L Sturkey, *Proc Phys Soc Lond* 80 (1962) 321–54.
[14] JA Kozubowski, WW Gerberich, and T Stefanski, *J Mater Res* 3 (1988) 710–13.
[15] DC Joy and DE Newbury, *J Mater Sci* 7 (1972) 714–16.
[16] S Villert, C Maurice, C Wyon, and R Fortunier, *Journal of Microscopy* 233 (2009) 290–301.
[17] A Winkelmann, *Ultramicroscopy* 108 (2008) 1546–50.
[18] A Bhattacharyya and JA Eades, *Scanning* 31 (2009) 114–21.

MT

the highest quality...
the most precise sectioning...
incomparable durability

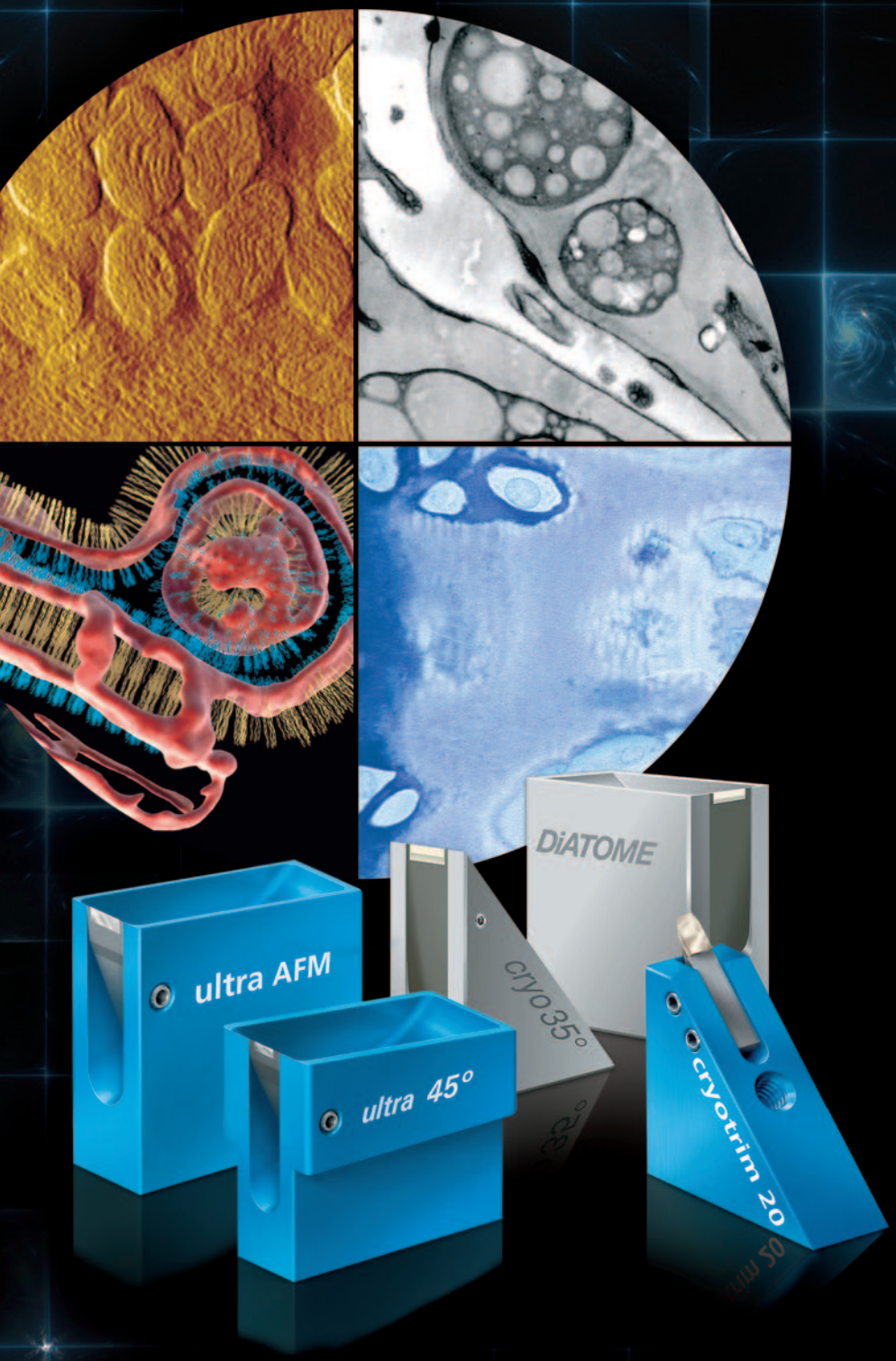

Free Customer Service

Sectioning tests with biological and material research specimens of all kinds. We send you the sections along with the surfaced sample, a report on the results obtained and a recommendation of a suitable knife. Complete discretion when working with proprietary samples.

Re-sharpening and Reworking Service

A re-sharpened Diatome diamond knife demonstrates the same high quality as a new knife. Even knives purchased in previous years can continue to be re-sharpened. The knives can be reworked into another type of knife for no extra charge, e.g. ultra to cryo or 45° to 35°.

Exchange Service

Whenever you exchange a knife we offer you a new Diatome knife at an advantageous price.

40 years of development, manufacturing, and customer service

DiATOME

diamond knives

ultra 45° • cryo • histo • ultra 35° • STATIC LINE II
cryo-P • cryo immuno • ultra sonic
cryotrim 45 and 25 ultra • AFM & cryo AFM • cryo 25°

DiATOME US • P.O. Box 550 • 1560 Industry Rd. • Hatfield, Pa 19440
Tel: (215) 412-8390 • Fax: (215) 412-8450 • email: sgkcck@aol.com • www.emsdiasum.com